

Hygrothermal Analysis of Most Common Historical Slabs in Hungary

Fanni Petresevics – Budapest University of Technology and Economics, Hungary – petresvics.fanni@emk.bme.hu

Balázs Nagy – Budapest University of Technology and Economics, Hungary – nagy.balazs@emk.bme.hu

Abstract

In Hungary and generally in Central Europe, a significant part of the existing building stock is constructed using traditional technologies that were widespread in the 19th and 20th centuries. Due to a lack of quality building materials, it was common practice to build structures using materials that were not specified and not following the prescribed layering scheme, so even a simple renovation project could typically be problematic. Moisture generated during the use of the building, condensation, and the initial construction moisture also have significant effects on building structures. In many cases, the reconstruction works are carried out due to a change of function, which can cause various external and internal moisture effects to affect the structure. To reduce the energy needs of the existing building stock, an increasing number of experts are starting to work on thermal and hygrothermal simulation of building structures. Numerical simulations of the distribution of humidity and temperature inside buildings can be used to determine the behavior of a building element during its life cycle, which can facilitate, among other things, the maintenance of architectural heritage and the design of renovations for energy efficiency. Within the framework of this research, detailed thermal and coupled heat and moisture transport simulations based on finite element methods were carried out to evaluate the energy performance of the most common traditional slab structures in Hungary. There were significant differences in both heat losses and thermal conductivity depending on whether only thermal or hygrothermal simulation was used and in general, hygrothermal simulations can provide much more accurate and detailed results. The simulations showed that none of the historic slab structures meet today's minimum energy and durability requirements, but with the suitable renovation method, heat losses for example, can be reduced by up to 25–60 %.

1. Introduction

By the late 19th century, Budapest had grown into a metropolis along with other Central European capitals, leading to a dramatic increase in the housing stock and multi-storey apartment blocks were built. In the early 1800s, wooden slabs and domes were the main horizontal load-bearing structures, replaced by bent steel beams later in the century. By the 1910s, reinforced concrete developed, and post-World Wars, prefabrication led to prestressed and formwork slab systems. Due to climate change and decreasing energy supplies, experts now focus on the thermal properties of buildings to reduce heat losses and maintenance costs. Recent changes in building energetics have been driven by technical progress and stricter regulations, increasing the need to reinforce and renovate existing structures. EU regulations require renovated structures to meet thermal standards, but 100-year-old slabs often fail to comply. Energy performance calculations must consider thermal bridges, described by linear thermal transmittance, while moisture bridges are also advised to be considered due to conservation reasons.

In the field of heat, air and moisture transport (HAM) in building and systems, much progress on the modeling and simulation tools has been established. However, the use of these tools in an integrated building simulation environment is still limited, since they mostly neglect or simplify building structures and thermal bridges. This is mainly caused by the lack of reliable thermophysical input data for building materials as well as by some intrinsic limitations in the simulation models, especially in describing the geometric features and peculiarities of the heritage buildings (Akkurt et al., 2020). Another issue is due to its long calculation

Part of

Pernigotto, G., Ballarini, I., Patuzzi, F., Prada, A., Corrado, V., & Gasparella, A. (Eds.). 2025. Building simulation applications BSA 2024. bu.press. <https://doi.org/10.13124/9788860462022>

time, since dynamic thermal analysis and HAM simulations are currently recommended only for research purposes (Nagy et al., 2022). Based on the research of the last years, it can even be said that the hygrothermal simulations of building elements and building structures (Sýkora et al., 2013), such as porous building materials (Abahri et al., 2011), solid masonry walls (Sýkora et al., 2009), prefabricated panels (Pihelo et al., 2016), insulated masonry or concrete (Ibrahim et al., 2014), lightweight concrete walls (Colinart et al., 2016), lightweight timber walls (McClung et al., 2014) or various cladding structures (Pihelo et al., 2016) are becoming more and more common. Less has been published on the hygrothermal analysis of building construction joints as wall-slab joints (Bianchi Janetti et al., 2012) and installation of openings (Nagy et al., 2018), which are largely responsible for thermal bridges according to Nagy (2019). Another less publicized topic is historic building structures (Cho et al., 2020; Gutland et al., 2022; Qin et al., 2024) and materials (Oumeziane et al., 2021; Jaros et al., 2023), even though urban modernization is progressing and the renovation of old buildings, especially historic buildings, is a priority for urban renewal.

This paper presents finite element simulations using COMSOL Multiphysics to compare thermal and moisture transmittances, including thermal bridges, of common slab structures (Prussian-, Monier-, Horcsik-, Bohn- and E-beam slab) under monthly design conditions, and to assess the impact of neglecting moisture transfer. Based on the performance of the analyzed slab types, renovation options were developed that can be of great help in practice. The results can be used and provide a reliable database for typology-based hygrothermal modeling of historic buildings and analysis based on dynamic simulations.

2. Methods

2.1 Numerical Model

Within the framework of this research, steady-state coupled heat and moisture transport simulations were performed by using Comsol Multiphysics 5.6 software, taking into account the latest EN

15026:2023 standard. The steady-state simulation was chosen instead of performing time-dependent hourly-based simulations because the main goal of the research was to compare surface, linear, and point thermal and moisture transmittances of the building constructions considering heating design conditions, and also to evaluate the effect of neglecting moisture transfer.

The first part of the partial differential equation (PDE) for steady-state heat transfer shown by Eq. (1) considers heat fluxes due to heat conduction, the second part takes into account heat fluxes due to evaporation.

$$\nabla q = \nabla[\lambda_{\text{eff}}\nabla T + L_v\delta_p\nabla(\varphi p_{\text{sat}}(T))] = 0 \quad (1)$$

If only a thermal simulation is performed on solids, only the first part is considered and given by Eq. (2).

$$q = -\lambda_{\text{eff}}\nabla T \quad (2)$$

In the case of steady-state moisture transfer, the PDE for solids is defined by Eq. (3), in which the first member of the equation represents the liquid transport of moisture fluxes, while the second part is responsible for moisture fluxes from vapor transport.

$$\nabla g = \nabla[\xi D_w\nabla\varphi + \delta_p\nabla(\varphi p_{\text{sat}}(T))] = G = 0 \quad (3)$$

The partial differential equations shown by Eq. (1) and Eq. (3) were implemented into COMSOL Multiphysics' Heat Transfer Module, which uses the EN 15026:2023 standard for HAM simulations.

2.2 Geometry

The geometric models of the analyzed 5 types of slabs were created and defined as solids in AutoCAD 2023, then exported in dwg to COMSOL Multiphysics. However, due to improved computational efficiency, simplifications were made in the geometry models. In the cases of PS and BS, the reinforcement was modeled separately as an octagonal prism instead of a cylinder, the reinforced slabs and ring beams were modeled with a higher equivalent thermal conductivity, and the coupling elements fixing the beams to the walls were neglected. To determine the heat losses of the wall surfaces and joints, 4 geometric models were made for each type of slab, giving a total of 20 models as follows: 2-way wall-slab corner connection, wall corner design,

wall-slab connection parallel and perpendicular to the load-bearing direction. The geometric model of the Prussian slab is shown in Fig. 1. Since all slab types are beam slabs, 2 beams, and 1.5 slab fields were considered in the modeling, and the length of the wall connections was determined according to EN ISO 10211:2017.

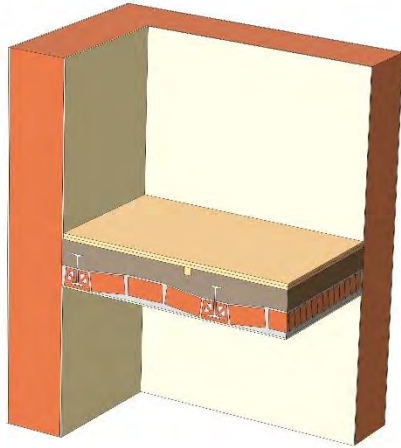


Fig. 1 - 2-way wall-slab corner connection of Prussian slab in COMSOL Multiphysics

2.3 Material Properties

With hygrothermal analysis, material properties that vary with temperature and moisture content can be considered, giving a better approximation of the real thermal behavior of materials. Material properties such as thermal conductivity, temperature and moisture dependent conversion factor, water vapor resistance factor were determined according to EN ISO 10456:2007, moisture storage curves and liquid transport coefficient were determined based on WUFI PRO 6.6 database. Table 1 shows the applied material properties, and Fig. 2 shows the sorption isotherms of the historical materials and materials of the renovation. While in the thermal simulations, the thermal conductivity of each material was given as a constant value as an input parameter, in the hygrothermal simulations it was calculated according to Eq. (6).

$$\lambda_{\text{eff}} = \lambda_1 * f_T * f_{\psi} \quad (6)$$

Table 1 – Applied material properties according to EN ISO 10456 and WUFI PRO 6.6 database

Material	λ_{eff} [W/mK]	f_T [1/K]	f_{ψ} [m ³ /m ³]	μ [-]	D_{w80} [m ² /s]	D_{100} [m ² /s]
plaster	0.80	0.001	4	10	1.09 $\times 10^{-10}$	2.49 $\times 10^{-8}$
fired clay	0.80	0.001	10	10	3.00 $\times 10^{-5}$	7.57 $\times 10^{-8}$
concrete	2.00	0.001	4	100	1.84 $\times 10^{-8}$	2.00 $\times 10^{-7}$
reinforced concrete	2.50	0.001	4	130	1.84 $\times 10^{-8}$	2.00 $\times 10^{-7}$
wood	0.18	1.400	80	5	4.00 $\times 10^{-12}$	5.00 $\times 10^{-12}$
slag fill	0.45	0.001	4	10	7.46 $\times 10^{-9}$	7.00 $\times 10^{-5}$
mortar	0.80	0.001	4	10	1.09 $\times 10^{-10}$	2.49 $\times 10^{-8}$
rebar	50.00	-	-	1000	-	-
mineral insulation	0.045	0.003	10	3	-	-
insulating plaster	0.05	0.001	4	10	-	-
internal plaster	0.155	0.001	4	10	-	-

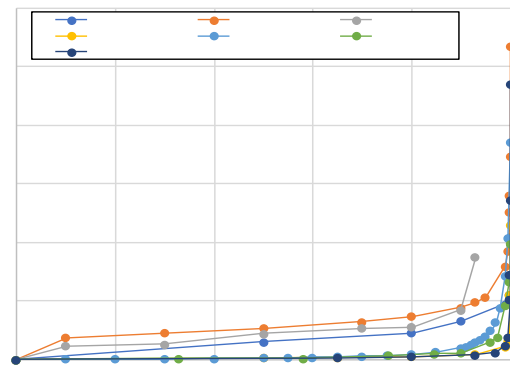


Fig. 2 – Sorption isotherms of applied materials

2.4 Boundary Conditions

When determining the boundary conditions of moisture transport, it is possible to use local weather data, therefore in this paper, the values are based on the research of Nagy (2019), which takes

into account the average January weather in Budapest. Internal conditions of air and equivalent vapor diffusion thicknesses of the boundary layers were set according to the EN 15026:2023. The temperatures were set to $T_{\text{int}} = 20$ °C for internal, $T_{\text{ext}} = 3.6$ °C for external. The external air and surface relative humidity were set to $\varphi_e = 0.74$ and $\varphi_{\text{se}} = 0.41$. The equivalent vapor diffusion thickness of the boundary layer was set to $s_{d,\text{si}} = 0.008$ m on the internal and $s_{d,\text{se}} = 0.0023$ m on the external surface. Surface heat transfer coefficients were set based on EN ISO 6946:2017. The heat transfer coefficients were set to $h_{\text{si}} = 7.69$ W/(m²K) for internal and $h_{\text{se}} = 25$ W/(m²K) for external surfaces.

2.5 Evaluation

Both thermal simulations and hygrothermal simulations were carried out to determine the point thermal transmittance and minimum temperature of the internal surfaces of the models. In the coupled heat and moisture transport simulations, the geometric models and material properties are the same as previously used in thermal simulations, but latent heat fluxes and the behavior of the materials against moisture were considered so that more accurate results can be expected. The heat losses can be used to determine the heat flux per m² of surface generated by a temperature difference of 1 K. The minimum temperature of the internal surface can be used to calculate the temperature factor which is useful when dealing with conservation problems. A calculation methodology according to EN ISO 10211:2017 was used.

To calculate the χ point thermal transmittance for the given structural design, the following Eq. (4) were used: L_{3D} were calculated for the junction, U_i thermal transmittance of the wall surfaces and Ψ_j linear thermal transmittances of the length of connections based on Eq. (4).

$$\chi = L_{3D} - \sum_{i=1}^{N_i} U_i * A_i - \sum_{j=1}^{N_j} \Psi_j * l_j \quad (4)$$

To check the durability and hygrothermal deterioration of the structures, the temperature factor is used for verification. According to DIN 4108-2:2010, if the value is less than 0.7, the design of the structures is inadequate and there is a risk of mold growth. f_{Rsi} temperature factor of the junctions can be calculated as follows on Eq. (5).

$$f_{\text{Rsi}} = \frac{T_{s,\text{min}} - T_e}{T_i - T_e} \quad (5)$$

3. Results and Discussion

The results have been evaluated by comparing surface, linear, and point thermal transmittances, and temperature factors in tabular and graphical form. Based on the methodology described in the previous chapter, the first step was to retrieve the temperature distribution, the total heat and moisture flux magnitude, and the relative humidity for each junction design from the numerical simulation. Due to the limitations of the presented paper, only relevant figures of one slab type (HS) are shown, but similar results are obtained for all slab types. The temperature distribution and the conductive heat flux magnitude of the 2-way wall-slab corner connection in case of only steady-state heat transfer considered are illustrated in Figs. 3-4. The temperature distribution and the total heat flux magnitude of the 2-way wall-slab corner connection of steady-state coupled heat and moisture simulation are shown in Fig. 5-6. In general, it is visible in all cases that there are large heat losses and thermal and moisture bridges, but typically these do not occur at the junction of the wall-joint but along the longitudinal joints of the wall-slab. This is partly because a decade ago, when most similar slab structures were built, there was no consideration of the need for a design that would be adequate in terms of durability, materials such as thermal insulation did not yet exist that could effectively reduce heat losses, and in many cases the knowledge of the material properties is uncertain. Comparing the result plots of thermal and hygrothermal simulations, we can see that both the temperature and the heat flux density distribution are similar, but the scaling of the plots is different, which means that different simulations lead to different results. These differences have been investigated in tabular and graphical form below in Figs. 7-10.

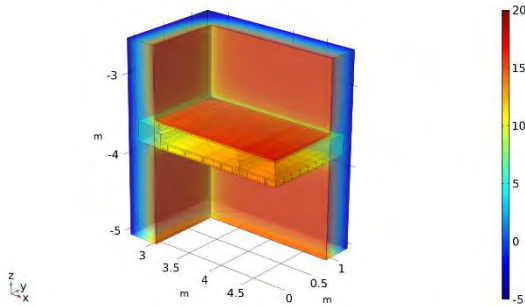


Fig. 3 – Temperature distribution [°C] of 2-way wall-slab corner connection of Horcsik-slab in case of thermal simulation

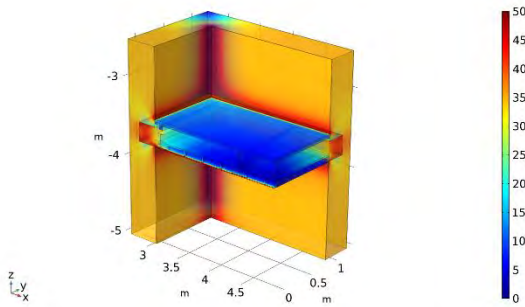


Fig. 4 – Heat flux magnitude [W/m²] of 2-way wall-slab corner connection of Horcsik-slab in case of thermal simulation

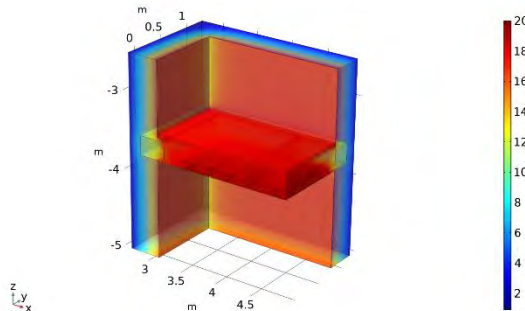


Fig. 5 – Temperature distribution [°C] of 2-way wall-slab corner connection of Horcsik-slab in case of hygrothermal simulation

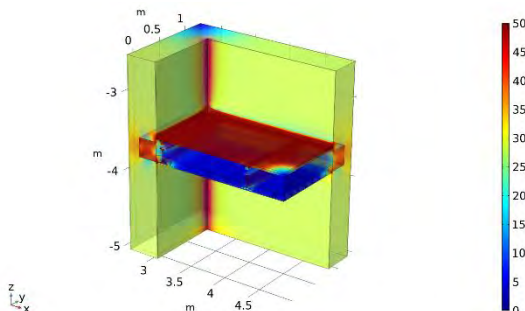


Fig. 6 – Heat flux magnitude [W/m²] of 2-way wall-slab corner connection of Horcsik-slab in case of hygrothermal simulation

Fig. 7-8 shows that the difference between the simulation results was more significant for the linear

thermal transmittance. It means the thermal bridges usually occur along the longitudinal joints of the wall-slab as previously shown in Figs. 3-6. and there is a risk of underestimating their magnitude if only thermal simulations are performed.

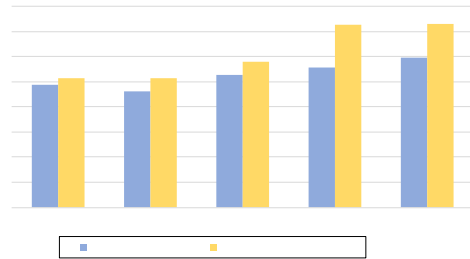


Fig. 7 – Comparison of Ψ_{2Dpar} parallel to the load-bearing direction of thermal and hygrothermal simulations

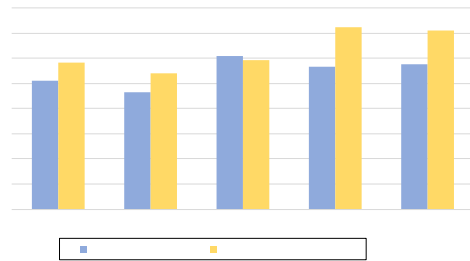


Fig. 8 – Comparison of Ψ_{2Dperp} perpendicular to the load-bearing direction of thermal and hygrothermal simulations

According to Fig. 9 MS and BS have such small heat losses that in these cases it is not necessary to perform 3D simulations to determine the heat losses of the junction. On the other hand, the HS and EBS have much higher excess heat losses at the junction, these slab types are designed with ring beams, so the large difference in the thermal conductivity of the materials also contributes to the higher heat losses. The negative value obtained for the PS means that the loss is only along the length of the wall-slab junction.

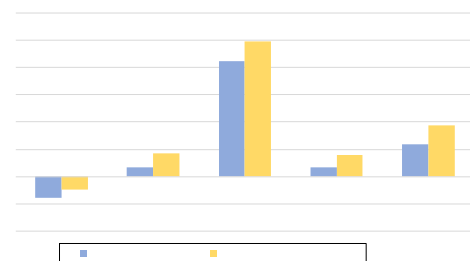


Fig. 9 – Comparison of χ of junction design of thermal and hygrothermal simulations

As seen in Fig. 10, the temperature factor based on hygrothermal simulations are below 0.7 (except for the hygrothermal simulation of MS), while the results of the thermal simulations for the PS, HS, and EBS are below 0.6., that means there is a high risk of mold growth. The lower values of thermal simulations are explained by the minimum temperatures of the internal surfaces being much lower than in the hygrothermal simulations and by the temperature difference between the external and internal surfaces being larger.

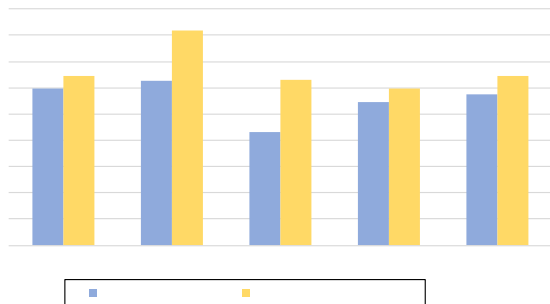


Fig. 10 – Comparison of f_{Rsi} of junction design of thermal and hygrothermal simulations

For thermal conductivity, only the main findings are presented in this article. The evaluation of the results shows that the results obtained from the hygrothermal simulation are always higher than the design values, but while in none of the cases do the wall, ceramic, and infill deviate by more than 5 % from the design values used in the thermal simulations, for the other materials the average thermal conductivity considered in the hygrothermal simulation can differ by up to 15–18 %.

Table 2 shows by what percentage the results of the hydrothermal simulations differ from the results of the thermal simulations. In most cases, if only thermal simulations are performed, this will lead to an underestimation of heat losses.

Table 2 – Differences between the results of thermal and hydrothermal simulation [%]

Case	PS	MS	HS	BS	EBS
Ψ_{2Dpar} [W/mK]	5,5 %	11,3 %	9,8 %	30,5 %	23,0 %
Ψ_{2Dperp} [W/mK]	14.5 %	16.3 %	-2.8 %	28.1 %	23.7 %
f_{Rsi} [°C]	8.0 %	30.8 %	45.6 %	9.6 %	12.3 %

χ [W/K] -40.3 % 160.6 % 16.7% 142.4 % 60.2 %

3.1 Design of Renovation for Energy Efficiency

As the results presented earlier show, none of the junction designs meet the energy and durability requirements. For listed buildings, renovation of the façade is generally not an option, therefore options with different thicknesses of internal thermal insulation and thermal insulation plaster were investigated. For each type of slab, at least 1 renovation option was developed based on hygrothermal simulations to achieve a temperature factor of 0.7 to meet the durability requirements, and the energy efficiency of the design was improved over the original condition.

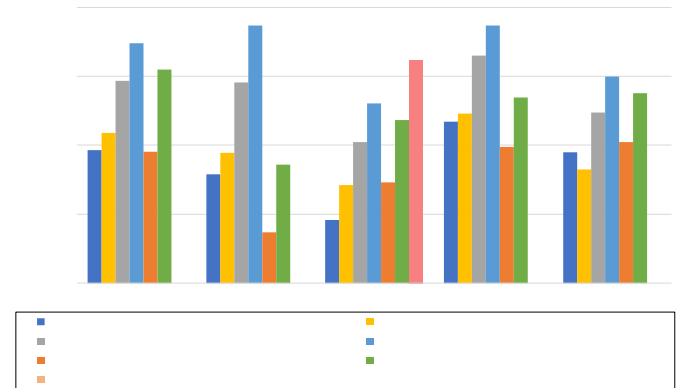


Fig. 11 – Comparison of f_{Rsi} for renovation options of different slabs

As shown in Fig. 11, the following renovation options were selected for each slab type to provide the requirements of durability:

- PS: 3-3 cm ext. and int. insulating plaster
- MS: 2-2 cm ext. and int. insulating plaster
- HS: 3-3 cm ext. and int. insulating plaster
- BS: 5 cm int. insulation with 2 cm plaster on the inside + 2 cm ext. insulation plaster
- EBS: 5 cm int. insulation with 1 cm plaster on the inside + 1 cm ext. insulation plaster

Although the thermal transmittance of the walls of listed buildings does not have to comply with the requirement ($U_{wall} \leq 0,24 \text{ W}/(\text{m}^2\text{K})$), the effectiveness of renovation options in reducing the U_{wall} has been investigated.

Based on Fig. 12, even 1 - 1 cm of insulation plaster on the inside and outside can significantly reduce U_{wall} by up to 35 %. Of course, the greatest reduction can be achieved by applying some form of thermal

insulation to both the inside and the outside, in this case, 5 cm of insulation on the inside and 2 cm of exterior insulation plaster can achieve a reduction of more than 70 %.

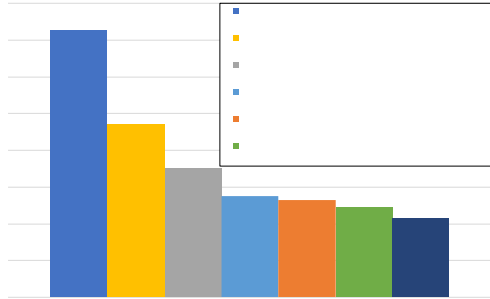


Fig. 12 – Comparison of U_{wall} for renovation options

4. Conclusion

One of the main tasks of the research is to investigate and develop options for energy-efficient retrofitting of the existing slab structures and create a reliable database for typology-based hygrothermal modeling of historic buildings and analysis based on dynamic simulation.

- Based on only 6 % difference between the results of thermal and hygrothermal simulation for the 3-dimensional thermal transmittance may lead to the conclusion that there is no need for 3D simulations, but the difference for the linear thermal transmittance (up to 30 %), the temperature factor (up to 45 %) and the heat losses (up to 160 %) was more significant.
- The deviation of the thermal conductivity from the design value is highly dependent on the material, since there are cases where the deviation is only 1-2 %, but there are also cases where the design value is 15 – 18 % less than the value obtained from the hygrothermal simulations.
- The results show that by choosing the most appropriate renovation method, heat losses, for example, can be reduced by up to 25 – 60 %. The best solution is to reduce the amount of heat fluxes on both the inside and the outside, so either we can apply thermal insulation on the inside with external insulating plaster or, for buildings that are not listed we can apply external thermal insulation.

One of the limitations was that standard material properties were considered, hence further research can be done to determine material properties in laboratory measurements specific to Hungary. By refining the models, extending the input physics, such as the consideration of airflow in the case of hollow slabs, and investigating more slab types, more comprehensive and complete results can be obtained.

Acknowledgement

The research reported here was supported by the TKP2021-NVA-02 project. Project no. TKP2021-NVA-02 has been implemented with the support provided by the Ministry of Innovation and Technology of Hungary from the National Research, Development and Innovation Fund, financed under the TKP2021-NVA funding scheme. Supported by the EKÖP-24-3 University Research Fellowship Programme of the Ministry for Culture and Innovation from the source of the National Research, Development and Innovation Fund.

Nomenclature

Symbols

$\nabla\left(\frac{\delta}{\delta x}, \frac{\delta}{\delta y}, \frac{\delta}{\delta z}\right)$	nabla vectorial diff. operator
q	heat flux [W/m^2]
λ_{eff}	temp. and vol. moist. cont. dependent thermal cond. [W/mK], based on EN ISO 10456
T	temperature [K]
L_v	latent heat of evaporation [J/kg]
$\delta_p = \delta_a/\mu$	vapor permeability [$\text{kg}/(\text{msPa})$]
δ_a	vapor permeability of still air depending on air temp. [$\text{kg}/(\text{msPa})$]
μ	water vapor resistance factor [1]
p_{sat}	sat. pressure of water vapor [Pa], depending on temp.
g	moisture flux
$\xi = \delta w/\delta \varphi$	diff. moist. capacity [kg/m^3]
w	moist. cont. [kg/m^3] according to the moist. stor. func. of the mat.
φ	relative humidity [-]
$\varphi_{\text{e, se}}$	ext. air and surface rel. humidity

λ	thermal conductivity [W/(m K)]
f_T	temp. dependent conv. factor [-]
f_ψ	moist. dependent conv. factor [-]
$D_{w,s}$	liquid transport coefficient [m ² /s]
$S_{d,s}$	equivalent vapor diffusion thickness [m]
h_s	heat transfer coefficient [W/(m ² K)]
χ	point thermal transmittance [W/K]
L_{3D}	3-D thermal transmittance [W/K]
U_i	thermal transmittance [W/(m ² K)]
A_i	interior surfaces [m ²]
$\Psi_{2Dperp/par}$	linear thermal transmittance perpendicular or parallel to the load-bearing direction [W/(m K)]
l_j	length of connections [m]
f_{Rsi}	temperature factor [-]
$T_{s,min}$	min. int. surface temperature [°C]

References

- Akkurt G., N. Aste, J. Borderon, A. Buda, M. Calzolari, D. Chung, and et. al, 2020 “Dynamic thermal and hygrometric simulation of historical buildings: Critical factors and possible solutions,” *Renew. Sustain. Energy Rev.*, vol. 118. <https://doi.org/10.1016/j.rser.2019.109509>
- Abahri K., R. Belarbi, and A. Trabelsi, 2011 “Contribution to analytical and numerical study of combined heat and moisture transfers in porous building materials,” *Build. Environ.*, vol. 46, no. 7, pp. 1354–1360. <https://doi.org/10.1016/J.BUILDENV.2010.12.020>.
- Bianchi Janetti M., F. Ochs, and R. Pfluger, 2012 “Coupling Forced Convection in Air Gaps with Heat and Moisture Transfer inside Constructions,” Proc. of the 2012 COMSOL Conf. in Milan, pp. 1-6
- Cho H., S. Yang, S. Wi, S. Chang, S. Kim, 2020 “Hygrothermal and energy retrofit planning of masonry façade historic building used as museum and office: A cultural properties case study” *Energy*, vol. 201, pp. 117607. <https://doi.org/10.1016/j.energy.2020.117607>
- Colinart T., D. Lelievre, and P. Glouannec, 2016 “Experimental and numerical analysis of the transient hygrothermal behavior of multilayered hemp concrete wall,” *Energy Build.*, vol. 112, pp. 1–11. <https://doi.org/10.1016/j.enbuild.2015.11.027>
- Gutland M., S. Bucking and M. Quintero, 2022 “Hygrothermal modelling of historic rubble masonry walls: Accounting for geometric and compositional variability” *Journal of Building Engineering*, vol. 48, pp. 103929. <https://doi.org/10.1016/j.jobe.2021.103929>
- Ibrahim M., E. Wurtz, and P. H. Biwole, 2014 “Hygrothermal performance of exterior walls covered with aerogel-based insulating rendering,” *Energy Build.*, vol. 132, pp. 241–251. <https://doi.org/10.1016/j.enbuild.2014.07.039>
- Jaroš P., M. Vertal, R. Slávik, 2023 “Hygric and thermal properties of Slovak building sandstones” *Journal of Building Engineering*, vol. 66, pp. 105891. <https://doi.org/10.1016/j.jobe.2023.105891>
- McClung R., H. Ge, J. Straube, and J. Wang, 2014 “Hygrothermal performance of crosslaminated timber wall assemblies with built-in moisture: field measurements and simulations,” *Energy Build.*, vol. 71, pp. 95–110. <https://doi.org/10.1016/j.buildenv.2013.09.008>
- Nagy B., 2019 “Designing insulation filled masonry blocks against hygrothermal deterioration,” *Engineering Failure Analysis*, vol. 103, pp. 144–157. <https://doi.org/10.1016/j.engfailanal.2019.05.005>
- Nagy B., M. Marosvölgyi, and Zs. Szalay, 2022 “Comparison of thermal bridge calculation,” *Acta Polytechnica CTU Proceedings* 38:77–83. <https://doi.org/10.14311/APP.2022.38.0077>
- Nagy B. and C. Tömböly, 2018 “Hygrothermal Analysis of Window Construction Joints,” *Zb. Rad. Građ. Fak.*, vol. 34, pp. 91–100. <https://doi.org/10.14415/konferencijaGFS2018.008>
- Oumeziane Y., A. Pierre, F. Mankibi et al., 2021 “Hygrothermal properties of an early 20th century clay brick from eastern France: Experimental characterization and numerical modeling” *Const. Build. Mat.*, vol. 273, pp. 121763. <https://doi.org/10.1016/j.conbuildmat.2020.121763>
- Pihelo P., H. Kikkas, and T. Kalamees, 2016 “Hygrothermal Performance of Highly Insulated Timber-frame External Wall,” *Energy*

- Procedia*, vol. 96, pp. 685–695.
<https://doi.org/10.1016/j.egypro.2016.09.128>
- Pihelo P., M. Lelumees, and T. Kalamees, 2016
“Influence of Moisture Dry-out on Hygrothermal Performance of Prefabricated Modular Renovation Elements,” *Energy Proc.*, vol. 96, pp. 745–755.
<https://doi.org/10.1016/j.egypro.2016.09.137>
- Qin X., H. Liu, X. Zhang, N. Jiang, L. Yang , 2024
“Thermal analysis of the window-wall interface for renovation of historical buildings” *Energy Build.*, vol. 310, pp. 114108.
<https://doi.org/10.1016/j.enbuild.2024.114108>
- Sýkora J., J. Vorel, T. Krejčí, M. Šejnoha, 2009
“Homogenization of coupled heat and moisture transport in masonry structures including interfaces” *Appl. Math. Comput.*, vol. 219, no. 13, pp. 7275–7285.
<https://doi.org/10.1016/j.amc.2011.02.050>
- Sýkora J., M. Šejnoha, and J. Šejnoha, 2013
“Homogenization of coupled heat and moisture transport in masonry structures including interfaces” *Appl. Math. Comput.*, vol. 219, no. 13, pp. 7275–7285.
<https://doi.org/10.1016/j.amc.2011.02.050>